
Research Article

A Novel Nanoparticle Formulation for Sustained Paclitaxel Delivery

W. J. Trickler,¹ A. A. Nagvekar,¹ and A. K. Dash^{1,2}

Received 4 October 2007; accepted 6 February 2008; published online 18 March 2008

Purpose. To develop a novel nanoparticle drug delivery system consisting of chitosan and glyceryl monooleate (GMO) for the delivery of a wide variety of therapeutics including paclitaxel.

Methods. Chitosan/GMO nanoparticles were prepared by multiple emulsion (o/w/o) solvent evaporation methods. Particle size and surface charge were determined. The morphological characteristics and cellular adhesion were evaluated with surface or transmission electron microscopy methods. The drug loading, encapsulation efficiency, *in vitro* release and cellular uptake were determined using HPLC methods. The safety and efficacy were evaluated by MTT cytotoxicity assay in human breast cancer cells (MDA-MB-231).

Results. These studies provide conceptual proof that chitosan/GMO can form polycationic nano-sized particles (400 to 700 nm). The formulation demonstrates high yields (98 to 100%) and similar entrapment efficiencies. The lyophilized powder can be stored and easily be resuspended in an aqueous matrix. The nanoparticles have a hydrophobic inner-core with a hydrophilic coating that exhibits a significant positive charge and sustained release characteristics. This novel nanoparticle formulation shows evidence of mucoadhesive properties; a fourfold increased cellular uptake and a 1000-fold reduction in the IC₅₀ of PTX.

Conclusion. These advantages allow lower doses of PTX to achieve a therapeutic effect, thus presumably minimizing the adverse side effects.

KEY WORDS: cancer; chitosan; GMO; MDA-MB-231; mucoadhesive; nanoparticles; paclitaxel.

INTRODUCTION

The localized or targeted delivery of chemotherapeutics has been exploited in recent trends to limit the indiscriminate toxicities to normal tissues associated with chemotherapy. Paclitaxel (PTX), the first of a new class of microtubule stabilizing agents, is recognized as an effective chemotherapeutic agent for a wide variety of solid tumors (1,2). Clinical application of this highly effective drug in the treatment of cancer is limited because of its poor aqueous solubility and poor oral bioavailability (3). To date, the only two commercial formulations have been developed. The first formulation developed uses 1:1 mixture of CremophorEL and ethanol to increase the solubility of paclitaxel administered intravenously (4). CremophorEL has been shown to have serious adverse side effects including severe hypersensitivity reactions, neurotoxicity, nephrotoxicity and hypotensive vasodilation (5–7). The newest advance in paclitaxel administration is an injectable suspension of albumin-bound paclitaxel nanoparticles called Abraxane has shown effective results (8,9).

However, bone marrow suppression is not only the dose dependant and dose limiting toxicity, but also neuropathy toxicity has been shown to be remarkably increased when compared to the traditional PTX formulation (10,11). Therefore, safe and effective drug delivery systems are needed to improve the safety and therapeutic efficacy of current clinical chemotherapeutic treatments.

Bioadhesive delivery systems are formulated to enhance drug bioavailability by increasing the residence time and subsequent absorption by the intimate contact of the drug delivery system (DDS) with the cellular surface. Chitosan has been shown to have bioadhesive properties due to interactions with the mucous membranes associated with epithelial barriers and tumors (12–15). Almost all human epithelial cell adenocarcinomas, nonepithelial cancer cell lines, hematological malignancies such as multiple myeloma, and some B-cell non-Hodgkin lymphomas exhibit an over expression of mucin-1 (16). Chitosan has been shown to have mucoadhesive properties both *in vitro* (12,15,17) and *in vivo* (13,18–21). Chitosan and glycerol monooleate (GMO) have been previously co-formulated together to sustain the delivery of PTX in an *in situ* gel with mucoadhesive properties (22). The current studies proposed to formulate a novel nanoparticulate delivery system (nDDS) consisting of chitosan/GMO for the delivery of a wide variety of drugs to overcome major obstacles like poor solubility, poor bioavailability and P-gp mediated efflux. This formulation proposes to overcome these obstacles through the bioadhesion of the nDDS. To

¹ Department of Pharmacy Sciences, School of Pharmacy and Health Professions, Creighton University Medical Center, 2500 California Plaza, Omaha, Nebraska 68178, USA.

² To whom correspondence should be addressed. (e-mail: adash@creighton.edu)

our knowledge, this is the first time these biomaterials have been co-formulated in a nanoparticle formulation.

The research reported here provides a proof of concept that these two biomaterials can be co-formulated to yield polycationic nano-sized particles, that typically range in diameter from 400 to 700 nm with the therapeutic agent entrapped, absorbed or chemically coupled in the biopolymeric matrices. The co-formulated chitosan/GMO nDDS provides bioadhesive properties to increase the cellular association of encapsulated drug and provide sustained release of the drug. In addition, the increased cellular association of encapsulated drug and sustained delivery corresponds to increased effectiveness of PTX in human breast cancer cells (MDA-MB-231). Together, the mucoadhesive properties of chitosan and the over expression of mucin-1 antigen in human adenocarcinomas may make a drug delivery system formulated with chitosan/GMO an ideal candidate for anti-cancer therapy.

MATERIALS AND METHODS

Materials

Paclitaxel (PTX) was purchased from InB:HauserPharmaceutical Services Inc. (Denver, CO, USA). MDA-MB-231 breast cancer cell line was purchased from American Type Culture Collection (ATCC; Manassas, VA, USA). The Gibco brand cell culture media and constituents, RPMI 1640, fetal bovine serum (FBS), penicillin/streptomycin, trypsin-EDTA and L-glutamine, were purchased from Invitrogen (Carlsbad, CA, USA). Glycerol monooleate (GMO) was obtained from Eastman Chemical Company (Kingsport, TN, USA). Anhydrous citric acid was purchased from Acros Organics (Fairlawn, NJ, USA). Acetonitrile (HPLC), methanol (HPLC), ammonium acetate (HPLC), sodium phosphate monobasic, sodium phosphate dibasic, hydrochloric acid (reagent grade), Triton-X-100, Thermanox® slides and Falcon tissue culture flasks and plates were purchased from Fisher Scientific (Fairlawn, NJ, USA). Tween-80 (T-80; polyoxyethylene sorbitan monooleate), and sodium chloride were purchased from Sigma Chemical Company (St. Louis, MO, USA). Low molecular weight chitosan was purchased from Aldrich Chemical Company (Milwaukee, WI, USA).

Preparation of Nanoparticles

In a typical procedure, the nDDS was prepared by a multiple oil-in-water emulsion and solvent evaporation method. GMO was melted (40°C) to achieve a fluid phase and an amount of either PTX (4.5% w/w/w), dexamethasone (DEX; 4.5% w/w/w) or osmium tetroxide (1.0% w/w/w; electron dense compound for transmission or scanning electron microscopy) was incorporated into the fluid phase of GMO (1.75 ml). An emulsion comprised of the GMO mixture (14% v/v) and an emulsifier (12.5 ml) consisting of 0.5% aqueous polyvinyl alcohol (mw 30,000–70,000) was ultrasonicated for 2 min at 18 W (Sonicator 3000, Misonix, Farmingdale, NY, USA). The oil-in-water emulsion thus formed was further emulsified in a solution (12.5 ml) of chitosan (2.4% w/v) dissolved in citric acid (100 mM) and ultrasonicated for 2 min at 18 W. The final multiple oil-water emulsion is frozen (−80°C) prior to freeze

drying (−52°C and <0.056 mBar pressure; FreeZone, Labconco, St Louis, MO, USA).

Nanoparticle Characterization

The mean particle size, size distribution and mean zeta potential of the nanoparticles were determined using a zetameter (ZetaPlus, Brookhaven Instruments Corporation, Holtsville, NY, USA). Briefly, the nanoparticles were resuspended in deionized water (0.4 mg/ml) in triplicate and analyzed for particle size and zeta potential. In addition, the particle size distribution and morphological microstructure were also visualized utilizing transmission electron microscopy (TEM) methods previously described (23). Briefly, the osmium tetroxide loaded nanoparticles were resuspended in deionized water (1 mg/ml) and placed (~20 µl) on Formvar®-coated copper grids (150 mesh, Ted Pella Inc., Redding, CA, USA) and allowed to air-dry at room atmospheric conditions. The dried grids were visualized using TEM (JEM-1011, Japan).

The percent nanoparticle yield was calculated by multiplying 100 to the ratio of weight of total lyophilized nanoparticulate powder yielded to total weight of all the formulation constituents used. The percent drug loading was calculated by multiplying 100 to the ratio of total amount of drug extracted from the polymeric matrix of a known weight of nanoparticles to the total weight of the nanoparticles used before extraction. The encapsulation efficiency was calculated by multiplying 100 to the ratio of weight of drug present in a batch of nanoparticle to the weight of drug (true amount) used in the formulation. Briefly, approximately 10 mg of accurately weighted lyophilized nanoparticles were dispersed in an organic solvent (15 ml, 60:40 v/v acetonitrile and water) and sonicated (Fisher Scientific FS 20, Fairlawn, NJ, USA) for 4 h to extract either PTX or DEX for HPLC analysis (Shimadzu SP-10A VP, Columbia, MD, USA). The HPLC analysis for PTX was achieved on a C18 Zorbax column (150×4.6 mm, 5 µm; Phenomenex, Torrance, CA, USA) with a mobile phase consisting of acetonitrile, methanol, 0.1M ammonium acetate (48.5:16.5:35% v/v/v) at a flow rate of 0.75 ml/min. The effluents were monitored at 227 nm and quantified using the area under the peak from standard solutions dissolved in mobile phase (0.4 to 2 µg/ml). The HPLC analysis for DEX was achieved on a C18 luna column (4.6 mm, 250 mm, 5 µm; Phenomenex, Torrance, CA, USA). The mobile phase for DEX was methanol/0.1 M ammonium acetate 60:40 (v/v) at flow rate of 1.2 ml/min. The effluents were monitored at 254 nm and quantified using the area under the peak from standard solutions dissolved in mobile phase (2 to 10 µg/ml).

The *in vitro* drug release profiles of different nanoparticle formulations were determined by measuring the cumulative amount of drug released from the nanoparticle over predetermined time intervals. Briefly, a known quantity of the formulation (2 mg) was dispersed in 40 ml of phosphate buffered saline (PBS; pH 7.4) in a capped Erlenmeyer flask in triplicate, agitated in a water bath incubator at 37°C and 80 rpm. At predetermined time intervals (5 to 240 min for PTX and 5 to 270 min for DEX), 200 µl of the sample was withdrawn with a filter tip needle and replaced with an equal amount of PBS. In simultaneous studies, equal amounts of the formulations were dispersed in 15 ml of acetonitrile/water

(60:40 *v/v*) and sonicated for 4 h to extract the total drug. In separate studies, the *in vitro* release of PTX was determined in the presence or absence of 0.02% (*v/v*) Tween-80 (T-80) by the same methods. The samples were suitably diluted before determining the drug concentration (PTX or DEX) by HPLC as previously described.

The physical state of the drug in the formulation was evaluated by x-ray powder diffractometry methods as previously described (24). Briefly, the blank nanoparticles and the nanoparticle formulations containing PTX or DEX were filled into a cavity-mount quartz holder. The samples were exposed to CuK-alpha radiation (40 kV and 30 mA) on an x-ray diffractometer (Rigaku D-Max/B Horizontal Q/2Q, Texas, USA). The nanoparticle formulations were also analyzed by differential scanning calorimetry (DSC). DSC thermograms were obtained for pure drugs, drug loaded nanoparticles, and blank nanoparticles. The lyophilized samples were weighed (3 mg) and sealed into aluminum crimp pans, and an empty pan was used as a reference. The samples were heated at the rate of 10°C/min, between 23 and 300°C in a DSC (Shimadzu DSC-60, Columbia, MD, USA) connected to a thermal data analysis system. The thermograms were analyzed after each run was performed.

The Cellular Association of Chitosan/GMO Nanoparticles

The *in vitro* bioadhesion and cellular uptake of the delivery system were evaluated in MDA-MB-231 human breast cancer cells. For the bioadhesion studies, MDA-MB-231 cells were seeded on Thermanox® cover-slips placed in falcon 6-well tissue culture plates at a density of approximately 150,000 cells per cover-slip and incubated for 24 h in a humidified chamber at 37°C in RPMI-1640 growth media supplemented with 10% FBS, 1% L-glutamine and 1% penicillin/streptomycin. Lyophilized osmium tetroxide loaded nanoparticles (1 mg/ml) were reconstituted in assay II buffer (122 mM sodium chloride, 3 mM potassium chloride, 25 mM sodium bicarbonate, 0.4 mM sodium phosphate di-basic, 1.4 mM calcium chloride, 1.2 mM magnesium sulfate, 10 mM HEPES, 10 mM glucose) adjusted to pH 7.4. The cell monolayers were exposed to the freshly dispersed osmium tetroxide nanoparticles for various times (15 to 30 min) in a humidified chamber at 37°C. After the exposure period, the cell monolayers were washed three times in ice cold PBS, fixed with a PBS buffered glutaraldehyde solution (3% *v/v*) and dehydrated with successive alcohol solutions (50% to 100%) for 10 min prior to mounting on a stub for critical point drying with carbon dioxide and gold sputter coating in an argon matrix for scanning electron microscopy (SEM) imaging. The mounted cell monolayers were visualized using SEM (JEOL-840A, Japan).

The cellular association of the nanoparticle delivery system in MDA-MB-231 human breast cancer cells was also analytically evaluated by the HPLC method previously mentioned. In these studies, the cell monolayers were cultured in standard 6-well tissue culture plates at a seeding density of 500,000 cells per square centimeter and cultured until confluency in a humidified chamber at 37°C in RPMI-1640 growth media supplemented with 10% FBS, 1% L-glutamine and 1% penicillin/streptomycin. Confluent cell monolayers were treated with a single bolus solution of paclitaxel (1 µM) or the

nanoparticulate delivery system loaded with paclitaxel (free fraction 1 µM) in assay buffer II for various times (15 to 45 min). The cell monolayers were washed three times with ice cold PBS and lysed with 1% triton-X-100. The cell monolayer lysates were collected in a microcentrifuge tube and a sample (25 µl) was assayed for total protein content by the Bradford colorimetric-analysis (BCA) protein assay (Pierce, Rockford, IL). The remaining cell lysates were frozen (-80°C) prior to freeze drying (-52°C and <0.056 mBar pressure; FreeZone, Labconco, Kansas City, MO, USA). The freeze dried cell monolayer lysates were re-suspended in acetonitrile, agitated at 100 rpm for 30 min at 37°C in an incubated shaker (Orbit, Labline Instruments Inc., Melrose Park, IL, USA). The microcentrifuge tubes were centrifuged at 14,000 rpm in a microcentrifuge for 5 min at 4°C (accuSpin Micro R, Fisher Scientific, Fairlawn, NJ, USA), and the amount of paclitaxel was determined in supernatant by HPLC methods. The cellular uptake was calculated as a ratio of the amount paclitaxel per mg total cellular protein.

The Cytotoxicity Profile of Chitosan/GMO Nanoparticles

The viability of MDA-MB-231 human breast cancer cells were determined using MTT cytotoxicity analysis. Briefly, the cells were seeded in a 24-well cell culture plate at a density of 20,000 cells per well in 1,000 µl of growth media and incubated overnight in a humidified chamber at 37°C in RPMI-1640 growth media supplemented with 10% FBS, 1% L-glutamine and 1% penicillin/streptomycin. The cells were treated with various concentrations (0.001 to 100 µM) in a single bolus with a solution of PTX or the nanoparticulate delivery system loaded with and without 4.5% (*w/w*) PTX (0.001 to 100 µM) or with 4.5% (*w/w*) dexamethasone (DEX; 0.001 to 100 µM) for 4 h, then washed three times with PBS (pH 7.4) and supplied with fresh growth media (48 to 96 h). After the incubation period, the cells were treated with fresh MTT reagent (250 µl, 5 mg/ml) and further incubated for 4 h, then treated with a fresh solvent consisting of 20% (*w/v*) SDS dissolved in water at 37°C mixed with an equal volume of DMF (dimethyl formamide). The solvent pH was adjusted to 7.4 using 2.5% of 80% acetic acid and 1% of 1 N HCl. The absorbance was read on a microplate reader at 550 nm. The absorbance data was analyzed and presented as percent survival of control monolayers receiving media alone.

Statistical Analyses

The results are expressed as means±standard error of the mean (SEM) for all quantitative data. The analytical cellular association data was statistically analyzed using single factor analysis of variance followed by Tukey multiple post hoc test for paired comparisons of means (SPSS 10, SPSS Inc., Chicago, IL, USA). For all studies, statistical significance was designated as $p < 0.05$, unless otherwise stated.

RESULTS AND DISCUSSIONS

Nanoparticle Characterization

The characteristics of chitosan/GMO nanoparticle formulations containing blank, PTX, DEX and osmium tetroxide

Table I. Physicochemical characterization of chitosan/GMO nanoparticles

Nanoparticle Preparation Chitosan/GMO	Particle Size (nm)	Particle Charge (mV)	Yield (%)	LE (%)	EE (%)
Blank	676.0±16.3	+31.78±0.54	99.7±0.17	n/d	n/d
Osmium tetroxide	532.2±39.3	+25.33±1.46	n/d	n/d	n/d
4.5% DEX	454.5±43.7	+26.66±0.87	99.4±0.32	4.5±0.05	99.5±0.17
4.5% PTX	432.5±37.1	+33.17±1.52	98.8±0.76	4.5±0.03	98.9±0.83

Values are mean±SEM; $n=3$
n/d not determined

ide are summarized in Table I. The mean particle size ranged from 676 nm (blank) to 435.5 nm (PTX). The mean size distribution appears to be inversely proportional to the hydrophobicity of the compound incorporated into the polymeric matrix suggesting that increasing the hydrophobicity of the drug encapsulated decreases the hydrodynamic volume of the nanoparticle by possibly tightly packing the hydrophobic tails of GMO. Although the mean particle size distribution decreased, there was no significant change in the surface charge distribution. The particle surface charge distribution ranged from 25.33 mV (osmium tetroxide) to 33.17 mV (PTX). The positive surface charge is indicative that chitosan is organized at the surface of the nanoparticle.

The mean percent yield was found to be near 100% with a low of 98.8 (PTX) to high of 99.7 (blank). The drug loading efficiency and encapsulation efficiency was also near 100% similar to the percent yield. De Campos and others have shown chitosan nanoparticles to have an entrapment efficiency of cyclosporine A, a hydrophobic drug like PTX, to be 74% (14). The entrapment efficiency of chitosan is dependant on many factors such as molecular weight of chitosan used, concentration of the drug molecules and pH of the formulation (25). Chitosan molecules basically interact with drug molecules by Van der Waals forces like electrostatic force, hydrogen bonding and hydrophobic interactions.

The encapsulation efficiency of chitosan nanoparticles has been shown to be inversely proportional to chitosan concentration and viscosity and drug concentration (25). To increase the loading efficiency of hydrophobic drugs and control the release of drug from various chitosan nanoparticle preparations, others have increased the hydrophobicity of chitosan with covalent modifications (26–30). Hu and colleagues (26) have used stearic acid grafted chitosan oligonucleotide self aggregated micelles to develop higher entrapment efficiencies (94%) for paclitaxel. In addition, Maestrelli and colleagues have shown that complexation of

hydrophobic drugs like furosemide with cyclodextrins increases their entrapment efficiency four- to tenfold in chitosan nanoparticles (29). Furthermore, studies by Prego and others have used solid triglycerides and polyethylene glycol (PEG) cores for chitosan surface modified nanocapsules to increase the loading efficiency (64% to 94%) of hydrophobic drugs for oral administration (31,32). Together, these studies indicate that the entrapment of hydrophobic drugs is not so efficient in chitosan nanoparticle preparations.

In the current study, the self-emulsifying properties of GMO formed a hydrophobic core, presumably micellar, to enhance the solubility of PTX and provide a foundation for chitosan aggregation. The near 100% loading and entrapment efficiencies of PTX in this formulation are attributed to the self-emulsifying properties of GMO. Monoglycerides, like GMO, are polar lipids with poor water solubility that exhibit properties that resemble non-ionic surfactants that have been comprehensively described (33).

Morphology and microstructure of the nanoparticles were examined using TEM (Fig. 1). The TEM images of the osmium tetroxide nanoparticles revealed a heterogeneous size distribution (Fig. 1). The nanoparticles also appear to suspend in an aqueous environment as individual particles with a spherical to elliptical shape. In addition, the absence of osmium tetroxide in the inner core of the nanoparticles suggests that the microstructure of the nanoparticles consists of a hydrophobic inner core consisting of GMO surrounded by a hydrophilic surface layer consisting of chitosan. The TEM images acquired at higher magnification show the particle surface morphology to be smooth and non-porous in nature suggesting that they may have a nano-sized gel

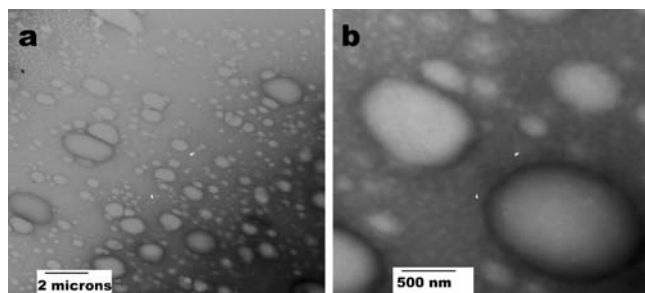


Fig. 1. Morphology and microstructure of chitosan/GMO nanoparticles. TEM images of osmium tetroxide loaded chitosan/GMO nanoparticles: **a** at magnification $\times 10,000$, and **b** at magnification $\times 50,000$

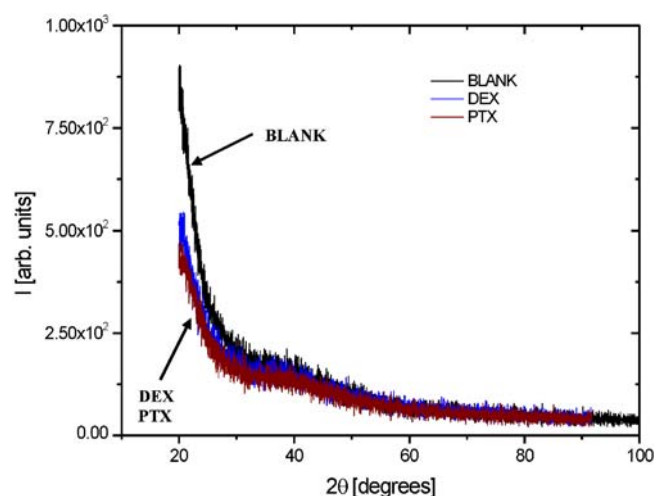


Fig. 2. X-ray Diffraction of blank chitosan/GMO nanoparticles compared to chitosan/GMO nanoparticles loaded with PTX or DEX

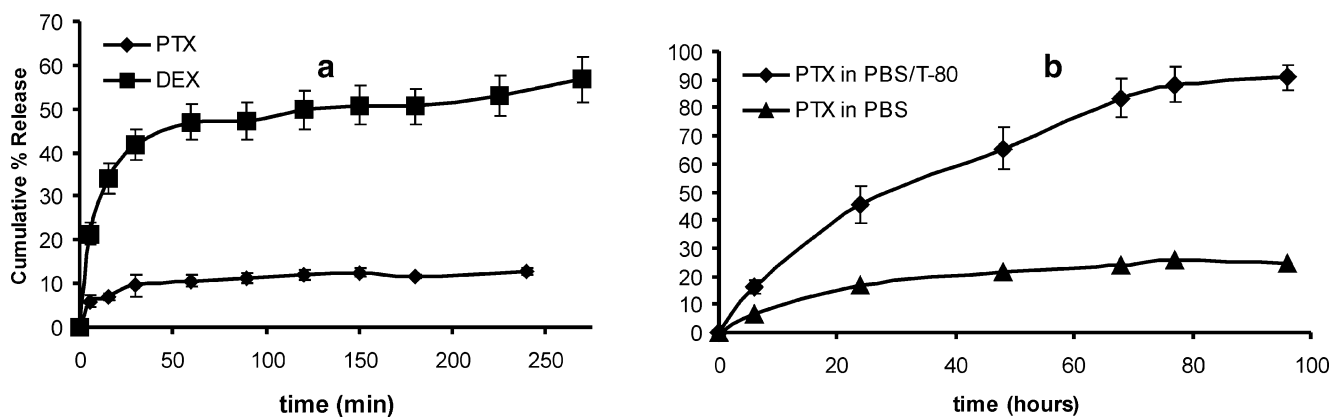


Fig. 3. The *in vitro* release profiles of PTX (closed diamonds) or DEX (closed squares) from chitosan/GMO nanoparticles into a release medium containing: **a** PBS without surfactant and **b** PBS with surfactant (0.02% [*v/v*] Tween-80)

forming nature in an aqueous environment (Fig. 1). Together, these data clearly provide evidence that nanoparticles consisting of chitosan/GMO can be lyophilized and reconstituted in an aqueous environment without distortion of shape and size.

The physical state of the drug in the polymeric matrix was examined using x-ray diffraction (Fig. 2). The powder x-ray diffraction pattern for the drug loaded nanoparticles was without any remarkable difference when compared to the powder x-ray pattern for blank nanoparticles. The lack of any remarkable diffraction patterns for the nanoparticles with PTX or DEX and without drug indicates that the drug incorporated in the nanoparticles existed in a non-crystalline state. The DSC Thermograms also provide further evidence by the lack of endothermic melting peaks for PTX (213°C) or DEX (262°C) in the nanoparticle formulations when compared to the crystalline drug alone (data not shown). In agreement with the powder x-ray pattern, the DSC thermographs further indicate that the drug incorporated in the nanoparticles existed in a non-crystalline state.

The *in vitro* drug release profiles of different nanoparticle formulations and the effects of Tween-80 were determined by measuring the cumulative amount of drug released from the nanoparticle over predetermined time intervals (Fig. 3). The *in vitro* drug release profiles for PTX and DEX showed common characteristics of burst-release initially followed by a slow release over the experimental period. A regression analysis of the slow terminal rate of drug release for the nanoparticles observed was approximately

0.013% per minute ($r^2=0.766$) with a maximal of 13% released in 4 h for PTX and 0.052% per minute ($r^2=0.922$) with a maximal of 55% released over a similar study period for DEX. The release profile suggests that under these conditions a single dose of chitosan/GMO nanoparticles loaded with PTX or DEX would, presumably, take an estimated 4.81 days or 18.4 h to release the entire entrapped drug from the formulation. In separate studies for a longer time period (96 h), the release characteristics of PTX from the chitosan/GMO nanoparticles were qualitatively similar when compared to the four hour study (Fig. 3). However, the presence of 0.02% (*v/v*) Tween-80 (T-80) increased the rate and extent of PTX released from the chitosan/GMO nanoparticle formulation (Fig. 3). The release characteristics of these drug delivery systems depend on the hydrophilicity or hydrophobicity of the drug incorporated and the water content of the medium. Monoglycerides like GMO have both hydrophobic and hydrophilic properties that have been extensively exploited as active drug delivery vehicles including liquid crystalline aggregates (liposomes and cubosomes) or cross-linked gel networks (hydrogels) (34–36). When the drug is incorporated in the lipid phase, the drug has to partition between the aqueous and the lipid phase, whereas drug entrapped in the aqueous channels of more complex structures would diffuse into the extracellular fluid. In the current studies, the chitosan/GMO nanoparticles demonstrated sustained release characteristics that appear to be dependent on the hydrophobicity of the therapeutic agent incorporated in the polymeric matrices. In well documented studies, the release of therapeutic agents from various polymeric matrices is dependant on concentration gradient, water penetration as well as structural degradation (37–40). In the current studies, the initial burst release of the therapeutic agent from chitosan/GMO nanoparticles is probably attributable to either surface bound moieties or tendency of chitosan to swell and in an aqueous environment permitting increased water penetration. However, the fact that extent and terminal rate of release for DEX was higher than PTX suggests the release mechanism of the therapeutic agent from chitosan/GMO nanoparticles depends on the partitioning of therapeutic agent from the hydrophobic core to the aqueous medium, since PTX is more hydrophobic than DEX. Further indications of this release mechanism are the increased rate and the increased extent of PTX released from the chitosan/GMO nanoparticles in the presence of a surfactant

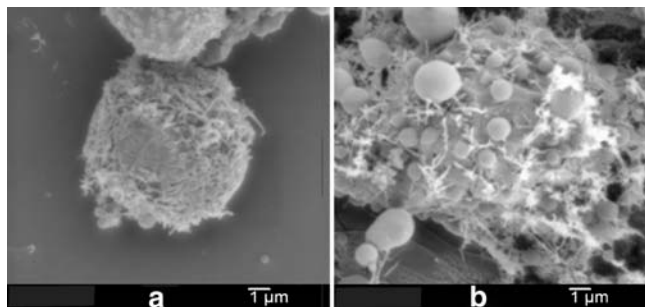


Fig. 4. The Bioadhesive properties of nanoparticles in MDA-MB-231 cells by SEM: **a** control cells treated with the particle suspension medium alone for 30 min, and **b** test cells treated with osmium tetroxide loaded nanoparticles for 30 min

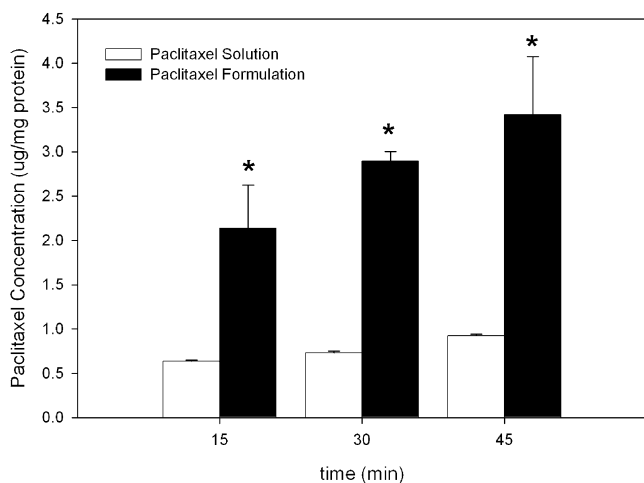


Fig. 5. The *in vitro* cellular association of nanoparticles loaded with PTX. Confluent MDA-231 monolayers exposed to paclitaxel solution (1 μ M, open bars) or nanoparticles containing paclitaxel (1 μ M free fraction, closed bars) at various time intervals

(T-80) increasing the water penetration. This mechanism of release suggests that the release characteristics could be further controlled by controlling the subsequent water penetration.

The Cellular Association of Chitosan/GMO Nanoparticles

The *in vitro* bioadhesion of the delivery system was evaluated in MDA-MB-231 human breast cancer cells (Fig. 4). The SEM micrographs of MDA-MB-231 cells treated in the vehicle alone show no remarkable nanoparticulate nodules when compared to monolayers treated with the chitosan/GMO nanoparticle formulation following 30 min of exposure (Fig. 4). The SEM micrograph confirmed the particle size and demonstrated the bio-adhesive properties of the chitosan/GMO formulations to the inherent negative cell surface-charge of the MDA-MB-231 cells (Fig. 4). The chitosan/GMO particles size distribution ranges from approximately 500 nm to around 1 μ m. This suggests the chitosan/GMO particles appear to be in a swollen hydrated state attached to the cellular surface. In addition, these data suggest that this formulation can adhere to the carbohydrates/glycoconjugate sites expressed on cancerous cells, and may have a preference for the over expressed mucopolysaccharides on the cell surface of cancerous cells. The idea of

bioadhesive properties have been of interest in the oral dosage forms of poorly absorbable drugs to adhere to the mucous membranes lining the gastrointestinal tract to increase the residence time. Studies by Takeuchi *et al.* have shown that chitosan coated liposomes to have mucoadhesive properties in an *in vitro* intestinal rat model (41). Additionally, Sandri and colleagues (15) demonstrated the mucoadhesion of a chitosan derivative (trimethylchitosan) and other chitosan delivery systems *in vitro* (Caco-2) and an ex vivo (rat jejunum) resulted in a prolonged residence time on intestinal mucosa offering a better chance for internalization.

The *in vitro* cellular association and uptake of the delivery system was further quantitatively evaluated in MDA-MB-231 human breast cancer cells (Fig. 5). The cellular association and uptake of paclitaxel was significantly increased with the nanoparticle formulation when compared to a solution of free paclitaxel throughout the entire study period. In addition, the increase in cellular association of PTX appears constant in a time dependent manner for both treatment groups. Furthermore, the increase was approximately fourfold higher in the chitosan/GMO formulation containing paclitaxel when compared to the free form of paclitaxel throughout the entire study period. The data is expressed as mean \pm SEM in Fig. 5 and considered statistically significant when **p* value is <0.05. The same mucoadhesive properties of chitosan have been shown effective in the delivery of various molecules in adenocarcinomas both *in vitro* and *in vivo* (13,18,42). Shikata and colleagues (42) demonstrated increased cellular internalization of drug loaded chitosan nanoparticles in squamous cell carcinomas (SCC-VII) and melanoma cells (B16F10) when compared to drug solutions alone. In agreement with these studies, the present study also provides evidence of the mucoadhesive properties of chitosan to human breast cancer cells (MDA-MB-231) *in vitro*. In addition to the mucoadhesive properties, the present study also demonstrated an increased cellular association of PTX when loaded into chitosan/GMO nanoparticles to MDA-MB-231 cells *in vitro*.

The Cytotoxicity Profile of Chitosan/GMO Nanoparticles

The MTT cytotoxicity dose-response studies revealed that the placebo (blank nanoparticles) \leq 1 mg/ml demonstrated a 100% cell-survival in MDA-MB-231 cells (Fig. 6). The dose-response studies further revealed that MDA-MB-231 cells exposed to the same dose (PTX solution versus amount

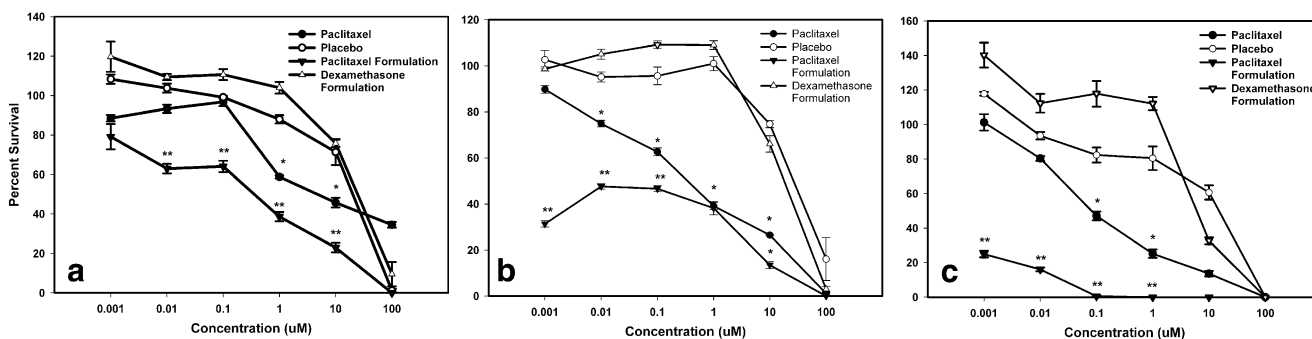


Fig. 6. The *in vitro* cytotoxicity effects of Chitosan/GMO nanoparticles in MDA-MB-231 cells at various times: **a** 48 h post-treatment, **b** 72 h post-treatment, and **c** 96 h post-treatment

released PTX from the formulation) of PTX for 4 h demonstrated a significant increase in cell death associated with the formulation when compared to PTX solution alone (Fig. 6). The fold IC₅₀ decrease for PTX formulation was approximately 650, 500, 1,000 at 48, 72 and 96 h post treatment when compared to the PTX solution (conventional therapy) alone (Fig. 6). The data was considered statistically significant when **p* value is <0.05 when compared to placebo or ***p* value <0.05 compared to paclitaxel solution and placebo. The significance of these data are that the bioadhesive and sustained delivery properties of the nanoparticulate formulation increases the residence time of the drug and thus, increases the duration of chemotherapeutic effect of PTX.

CONCLUSION

In conclusion, this work provides conceptual proof and a foundation that chitosan/GMO can form polycationic nano-sized particles with high yields, entrapment efficiencies and sustained release characteristics. Furthermore, the chitosan/GMO nanoparticles show evidence of significant mucoadhesive properties, increased cellular association and presumably intercellular internalization in MDA-MB-231 cells. These advantages allow lower doses of PTX to achieve an efficacious therapeutic window, and thus, minimizing the adverse side effects associated with chemotherapeutics like PTX.

ACKNOWLEDGEMENTS

These studies were supported by a Department of Defense Concept Award BC045664.

REFERENCES

1. J. A. Ajani, *et al.* Phase II study of Taxol in patients with advanced gastric carcinoma. *Cancer J. Sci. Am.* **4**(4):269–274 (1998).
2. B. B. Rogers. Taxol: a promising new drug of the '90s. *Oncol. Nurs. Forum* **20**(10):1483–1489 (1993).
3. A. K. Singla, *et al.* Paclitaxel and its formulations. *Int. J. Pharm.* **235**(1–2):179–192 (2002).
4. B. D. Tarr, and S. H. Yalkowsky. A new parenteral vehicle for the administration of some poorly soluble anti-cancer drugs. *J. Parenter. Sci. Technol.* **41**:31–33 (1987).
5. T. C. Chao, *et al.* Paclitaxel in a novel formulation containing less Cremophor EL as first-line therapy for advanced breast cancer: a phase II trial. *Invest. New Drugs* **23**(2):171–177 (2005).
6. H. Gelderblom, *et al.* Cremophor EL: the drawbacks and advantages of vehicle selection for drug formulation. *Eur. J. Cancer* **37**(13):1590–1598 (2001).
7. D. Friedland, *et al.* Hypersensitivity reactions from taxol and etoposide. *J. Natl. Cancer Inst.* **85**(24):2036 (1993).
8. N. K. Ibrahim, *et al.* Phase I and pharmacokinetic study of ABI-007, a Cremophor-free, protein-stabilized, nanoparticle formulation of paclitaxel. *Clin. Cancer Res.* **8**(5):1038–1044 (2002).
9. W. J. Gradishar. Albumin-bound paclitaxel: a next-generation taxane. *Expert Opin. Pharmacother.* **7**(8):1041–1053 (2006).
10. M. Socinski. Update on nanoparticle albumin-bound paclitaxel. *Clin. Adv. Hematol. Oncol.* **4**(10):745–746 (2006).
11. J. Lee Villano, *et al.* Abraxane induced life-threatening toxicities with metastatic breast cancer and hepatic insufficiency. *Invest. New Drugs* **24**(5):455–456 (2006).
12. A. Bernkop-Schnurch, *et al.* Thiomers: preparation and *in vitro* evaluation of a mucoadhesive nanoparticulate drug delivery system. *Int. J. Pharm.* **317**(1):76–81 (2006).
13. F. Zheng, *et al.* Chitosan nanoparticle as gene therapy vector via gastrointestinal mucosa administration: results of an *in vitro* and *in vivo* study. *Life Sci.* **80**(4):388–396 (2007).
14. A. M. De Campos, *et al.* Chitosan nanoparticles: a new vehicle for the improvement of the delivery of drugs to the ocular surface. Application to cyclosporin A. *Int. J. Pharm.* **224**(1–2):159–168 (2001).
15. G. Sandri, *et al.* Nanoparticles based on *N*-trimethylchitosan: evaluation of absorption properties using *in vitro* (Caco-2 cells) and *ex vivo* (excised rat jejunum) models. *Eur. J. Pharm. Biopharm.* **65**(1):68–77 (2007).
16. A. Moore, *et al.* *In vivo* targeting of underglycosylated MUC-1 tumor antigen using a multimodal imaging probe. *Cancer Res.* **64**(5):1821–1827 (2004).
17. F. Cui, *et al.* Preparation and characterization of mucoadhesive polymer-coated nanoparticles. *Int. J. Pharm.* **316**(1–2):154–161 (2006).
18. K. A. Howard, *et al.* RNA interference *in vitro* and *in vivo* using a novel chitosan/siRNA nanoparticle system. *Mol. Ther.* **14**(4):476–484 (2006).
19. H. Takeuchi, *et al.* Enteral absorption of insulin in rats from mucoadhesive chitosan-coated liposomes. *Pharm. Res.* **13**(6):896–901 (1996).
20. H. Takeuchi, *et al.* Novel mucoadhesion tests for polymers and polymer-coated particles to design optimal mucoadhesive drug delivery systems. *Adv. Drug Deliv. Rev.* **57**(11):1583–1594 (2005).
21. J. Thongborisute, *et al.* The effect of particle structure of chitosan-coated liposomes and type of chitosan on oral delivery of calcitonin. *J. Drug Target* **14**(3):147–154 (2006).
22. S. Jauhari, and A. K. Dash. A mucoadhesive *in situ* gel delivery system for paclitaxel. *AAPS PharmSciTech.* **7**(2):E53 (2006).
23. J. Panyam, and V. Labhasetwar. Targeting intracellular targets. *Curr. Drug Deliv.* **1**(3):235–247 (2004).
24. A. K. Dash, *et al.* X-ray powder diffractometric method for quantitation of crystalline drug in microparticulate systems. I. Microspheres. *J. Pharm. Sci.* **91**(4):83–990 (2002).
25. Y. Wu, *et al.* Chitosan nanoparticles as a novel delivery system for ammonium glycyrrhizinate. *Int. J. Pharm.* **295**(1–2):235–245 (2005).
26. F. Q. Hu, *et al.* Shell cross-linked stearic acid grafted chitosan oligosaccharide self-aggregated micelles for controlled release of paclitaxel. *Colloids Surf. B Biointerfaces* **50**(2):97–103 (2006).
27. J. Hyung Park, *et al.* Self-assembled nanoparticles based on glycol chitosan bearing hydrophobic moieties as carriers for doxorubicin: *in vivo* biodistribution and anti-tumor activity. *Biomaterials* **27**(1):119–126 (2006).
28. J. H. Kim, *et al.* Hydrophobically modified glycol chitosan nanoparticles as carriers for paclitaxel. *J. Control Release* **111**(1–2):228–234 (2006).
29. F. Maestrelli, *et al.* A new drug nanocarrier consisting of chitosan and hydroxypropylcyclodextrin. *Eur. J. Pharm. Biopharm.* **63**(2):79–86 (2006).
30. S. A. Agnihotri, *et al.* Recent advances on chitosan-based micro- and nanoparticles in drug delivery. *J. Control Release* **100**(1):5–28 (2004).
31. C. Prego, *et al.* Chitosan-PEG nanocapsules as new carriers for oral peptide delivery. Effect of chitosan pegylation degree. *J. Control Release* **111**(3):299–308 (2006).
32. M. Garcia-Fuentes, *et al.* A comparative study of the potential of solid triglyceride nanostructures coated with chitosan or poly(ethylene glycol) as carriers for oral calcitonin delivery. *Eur. J. Pharm. Sci.* **25**(1):133–143 (2005).
33. E. S. Lutton. Phase behavior of aqueous systems of monoglycerides. *J. Am. Oil Chem. Soc.* **42**(12):1068–1070 (1965).
34. G. Garg, and S. Saraf. Cubosomes: an overview. *Biol. Pharm. Bull.* **30**(2):350–353 (2007).

35. S. Ganguly, and A. K. Dash. A novel *in situ* gel for sustained drug delivery and targeting. *Int. J. Pharm.* **276**(1–2):83–92 (2004).
36. Y. Sadhale, and J. C. Shah. Glyceryl monooleate cubic phase gel as chemical stability enhancer of cefazolin and cefuroxime. *Pharm. Dev. Technol.* **3**(4):549–556 (1998).
37. M. Uner. Preparation, characterization and physico-chemical properties of solid lipid nanoparticles (SLN) and nanostructured lipid carriers (NLC): their benefits as colloidal drug carrier systems. *Pharmazie* **61**(5):375–386 (2006).
38. P. M. Bummer. Physical chemical considerations of lipid-based oral drug delivery—solid lipid nanoparticles. *Crit. Rev. Ther. Drug Carrier Syst.* **21**(1):1–20 (2004).
39. P. R. Lockman, *et al.* Nanoparticle technology for drug delivery across the blood–brain barrier. *Drug Dev. Ind. Pharm.* **28**(1):1–13 (2002).
40. S. J. Douglas, *et al.* Nanoparticles in drug delivery. *Crit. Rev. Ther. Drug Carrier Syst.* **3**(3):233–261 (1987).
41. H. Takeuchi, *et al.* Mucoadhesive nanoparticulate systems for peptide drug delivery. *Adv. Drug Deliv. Rev.* **47**(1):39–54 (2001).
42. F. Shikata, *et al.* *In vitro* cellular accumulation of gadolinium incorporated into chitosan nanoparticles designed for neutron-capture therapy of cancer. *Eur. J. Pharm. Biopharm.* **53**(1):57–63 (2002).